Bioactive Cinchona Alkaloids from Remijia peruviana

ARTICLE *in* JOURNAL OF AGRICULTURAL AND FOOD CHEMISTRY · APRIL 2005

Impact Factor: 2.91 · DOI: 10.1021/jf048880e · Source: PubMed

JOURNAL OF AGRICULTURAL AND FOOD CHEMISTRY

Bioactive *Cinchona* Alkaloids from *Remijia peruviana*

LASTENIA RUIZ-MESIA,[†,‡] WILFREDO RUIZ-MESÍA,[†] MATÍAS REINA,*[,§] RAFAEL MARTÍNEZ-DIAZ,[||] CONCEPCIÓN DE INÉS,[⊥] ANA GUADAÑO,[⊥] AND AZUCENA GONZÁLEZ-COLOMA[⊥]

Instituto de Productos Naturales y Agrobiología (IPNA), CSIC, La Laguna, Tenerife, Spain, Laboratorio de Productos Naturales, Facultad de Ingeniería Química, Universidad Nacional de la Amazonía Peruana (UNAP), Iquitos, Perú, Universidad Autónoma de Madrid (UAM), Spain, Centro de Ciencias Medioambientales (CCMA), CSIC, Madrid, Spain, and Instituto de Investigación de la Amazonía Peruana (IIAP), Iquitos, Perú

Three known *Cinchona* alkaloids of the quinine type, quinine (**1**), cupreine (**2**), cinchonine (**3**), and the possible artifact cinchonine−HCl (**3**−HCl), along with two new ones, acetylcupreine (**4**) and *N*-ethylquinine (**5**), have been isolated from the bark of *Remijia peruviana* (Rubiaceae). Their stereochemical structures were established by high resolution NMR spectroscopy. Alkaloids **2**−**4** had antifeedant effects on *Leptinotarsa decemlineata* with varying potencies. Compound **4** was cytotoxic to both insect Sf9 and mammalian CHO cells after 48 h of incubation, while **3**−HCl had stronger and selective cytotoxicity to Sf9. Quinine **1** had a moderate to low effect on *Trypanosoma cruzi*. Tumoral cells were also affected by these alkaloids, with **4** and **3**−HCl being the most cytotoxic to all the cell lines tested. Overall, the 8*R*, 9*S* configurations, as in **3** and **3**−HCl**,** as well as the C-6′ acetylated alkaloid **4**, with an 8*S*, 9*R* configuration, showed stronger biological effects.

KEYWORDS: ***Remijia peruviana* (Rubiaceae); *Cinchona* alkaloids; structural elucidation; acetylcupreine; *N*-ethylquinine; antifeedant effects; *Spodoptera littoralis*; *Leptinotarsa decemlineata*; trypanocidal; cytotoxic activity**

INTRODUCTION

Cinchona alkaloids isolated from the bark of several species of *Cinchona* and *Remijia* trees have been extensively studied for their antimalarial and antiarrythmic properties (*1*, *2*). These molecules are composed of two relatively rigid entities: an aromatic quinoline ring and an aliphatic quinuclidine ring connected by two carbon−carbon single bonds differing only in their configuration at the C-8 and C-9 positions (*3*). The unequivocal assignments of the stereochemical structures of these alkaloids have been established by NMR (*4*).

The shrub *Remijia peruviana* Standley (Rubiaceae), known locally as "*cascarilla*", was studied as part of an ongoing program to investigate the medicinal properties and ecological role of *Cinchona* alkaloids. This plant is found in the Peruvian Amazonian forest, and the bark is used in popular medicine as an antimalarial remedy (*5*).

In this work, the known alkaloids quinine (**1**), cupreine (**2**), and cinchonine (**3**) and the new alkaloids acetylcupreine (**4**) and *N*-ethylquinine (**5**) have been isolated. The structures of these alkaloids were established by spectroscopic methods, and the complete ^{1}H and ^{13}C shift assignments of the new alkaloids based on 2D NMR experiments are reported.

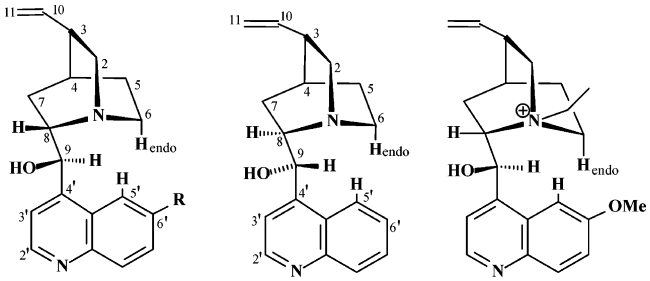

1 R = OMe
2 R = OH
4 R = OAc

3

5

The plant's defensive properties (insect antifeedant and toxic effects) of alkaloids **1**−**4** (compound **5** was not available for the biological tests) were investigated against *Spodoptera littoralis*, *Leptinotarsa decemlineata*, and *S. frugiperda* pupal ovarian tissue cells (Sf9). Additional pharmaceutical properties of these alkaloids have been investigated by testing their trypanocidal effects on epimastigote forms of *Trypanosoma cruzi* and their cytotoxic effects on mammalian chinese hamster ovary (CHO) cells and a panel of tumor cell lines with different

* To whom correspondence should be addressed. Phone: 34 922 256847. Fax: 34 922 260135. E-mail: mreina@ipna.csic.es.
[†] UNAP.
[‡] IIAP.
[§] IPNA.
[||] UAM.
[⊥] CCMA.

10.1021/jf048880e CCC: $30.25
Published on Web 02/23/2005

resistance mechanisms. Murine colon adenocarcinoma (CT26) expresses low levels of P-glycoprotein (Pgp), the multidrug-resistance protein (MRP1), and the murine glutathione/glutathione *S*-transferase detoxification system (GSH/GST) (*6*, *7*); human colon adenocarcinoma (SW480) has elevated levels of Pgp (*8*) with low levels of MRP1 and the g-glutamylcysteine synthetase (g-GCS) (*9*) responsible for *de novo* synthesis of GSH; human cervical adenocarcinoma (HeLa) express intermediate levels of GSH-conjugate export activity (*10*); human melanoma (SkMel25) expresses low invasive and metastatic potential (*11*); and human malignant melanoma (SkMel28) expresses GSHpx and GSTs (*12*) and low levels of MRP1 (*13*).

MATERIALS AND METHODS

General. Melting points were determined on a Reichert Thermovar apparatus and are uncorrected. Optical rotations were determined in EtOH at room temperature using a Perkin-Elmer 137 polarimeter. IR and UV spectra were taken on a Perkin-Elmer 1600 FT and a Varian Carey 1E spectrometer, respectively. NMR spectra were measured on a Bruker AMX2 500 MHz spectrometer with a pulsed field gradient using the solvent as an internal standard ($CDCl_3$, at δ_H 7.26 and δ_C 77.0). The programs used in two-dimensional (2D) NMR experiments (HMBC, HSQC, correlation spectroscopy (COSY), and nuclear Overhauser enhancement spectroscopy (NOESY)) were those furnished with the manufacturer's software. EIMS and exact mass measurements were recorded on a Micromass Autospec instrument at 70 and 15 eV. Elemental analyses were determined on a Fisons Instruments EA 1108 CHN. Silica gel (Merck 15111, 7741) and alumina (Aldrich 19944-3 and Merck 5550) were used for column chromatography and TLC. Alkaloids were visualized by thin-layer chromatography (TLC) with Dragendorff's reagent. RPMI 1640, fetal bovine serum (FBS), L-glutamine, and penicillin/streptomycin were from GIBCO-BRL (United Kingdom). 3-[4,5-Dimethylthiazol-2-yl]-2,5-diphenyl-tetrazolium bromide (MTT) and *p*-nitrophenyl phosphate were from Sigma-Aldrich.

Plant Material. Bark of *Remijia peruviana* Standley was collected from adult flowering trees in November of 1994 near the Pañacocha community (12 km from Iquitos, Perú, 120 m above sea level) and identified by Ing. J. Ruiz Macedo. A voucher specimen (no. 5402) has been deposited in the Herbarium of the Universidad Nacional de la Amazonia Peruana, Iquitos, Perú.

Insect Bioassays. *S. littoralis* and *L. decemlineata* colonies were reared on artificial diet and potato (*Solanum tuberosum* L) plants, respectively, and maintained at 22 + 1 °C and >70% relative humidity with a photoperiod of 16:8 h (L:D) in a growth chamber.

Choice Feeding Assay. These experiments were conducted with sixth-instar *S. littoralis* larvae and *L. decemlineata* adults. Percent feeding inhibition (%FI) was calculated as described by Reina et al. (*14*). Compounds with a FI of >50% were tested in a dose−response experiment to calculate their relative potency (EC_{50} values, the effective dose for 50% feeding reduction), which was determined from linear regression analysis (%FI on log dose).

Oral Cannulation. This experiment was performed with preweighed newly molted *S. littoralis* L6 larvae as previously described (*15*). An analysis of covariance (ANCOVA) on biomass gains with initial biomass as covariate (covariate $p > 0.05$) showed that initial insect weights were similar among all treatments. A second ANCOVA analysis was performed on biomass gains with food consumption as covariate to test for postingestive effects.

Trypanocidal Activity. This activity was assayed on epimastigote forms of *T. cruzi*, Y strain, as described in González-Coloma et al. (*15*). Parasite viability was analyzed by a modified MTT colorimetric assay method (*16*). The activity was calculated as % growth inhibition. ED_{50} values were determined for each compound as the effective dose to produce 50% growth inhibition, which was determined from linear regression analysis (% growth inhibition on log dose).

Cytotoxicity. Sf9 insect cells (European Collection of Cell Cultures (ECCC)), CHO mammalian cells (Dr. Pajares, Instituto de C. Biomédicas, CSIC), and the tumoral cell lines (Deutsches Krebsforschungszentrum (DKFZ)) CT26, SW480, HeLa, SkMel25, and SkMel28 were cultured as previously described (*15*). Cell viability was analyzed by an adaptation of the MTT colorimetric assay method (*17*−*19*) and the relative potency of the active compounds (ED_{50}, effective dose to give 50% cell viability) calculated as previously described (*15*). In brief, cells in the logarithmic growth phase were added to 96-well flat-bottom microtiter plates at a density of 2.5×10^3 cells/well for CHO, CT26, SW480, and SkMel28 cells and 5×10^3 cells/well for HeLa cells and incubated for 6 days with different concentrations of the compounds dissolved in absolute ethanol. This time of incubation was used to predict the possible adverse cytotoxic effects of compounds on CHO cells. In all cases, the viability of the cells treated under the same conditions with the residual concentration of solvents was ≥95%.

Extraction and Isolation. A sample (1.5 kg) of dry ground plant bark was treated with 5% citric acid for 48 h. The acidic solution (pH 2) was extracted with $CHCl_3$ to yield a non-alkaloidal crude extract (65 mg). The aqueous phase was basified to pH 10 with a saturated solution of NaOH and extracted with CH_2Cl_2 to yield a crude alkaloidal extract (2.15 g). This crude extract was chromatographed over alumina oxide 90 (Activity II) with mixtures of increasing polarity of *n*-hexane/EtOAc−MeOH to give fractions A (12.5 mg), B (99.5 mg), C (53.1 mg), D (53.1 mg), E (35.0 mg), F (12.6 mg), G (185.6 mg), H (182.0 mg), I (45.7 mg), J (25.8 mg), K (32,1 mg), and L (348,6 mg). Further purification of fractions D, E, F, G, and H on alumina eluted with EtOAc−MeOH gradients yielded alkaloids **1**−**5**.

Acetylcupreine (**4**). Amorphous white powder; $[\alpha]^{25}_D$ − 116.6° (*c* 0.325, EtOH); IR (film) ν_{max}: 2960, 1620, 1574, 1556, 1470, 1404, 1241, 1133, 982, 753 cm^{-1}; UV (EtOH) λ_{max} (log ϵ) 336 sh (2.48) nm, 286 sh (2.41) nm, 232 (3.25) nm; EIMS *m*/*z* $[M]^+$ 352 not detectable, 324 (1), 309 (2), 294 (1), 175 (6), 159 (3), 145 (4), 137 (10), 136 (100), 95 (86), 81 (13), 55 (9); HRMS *m*/*z* $[M]^+$ 352.1775 (calcd for $C_{21}H_{24}N_2O_3$ 352.1786). Anal. Calcd for $C_{21}H_{24}N_2O_3$: C, 71.59; H, 6.80; N, 7.90. Found: C, 71.30; H, 7.41; N, 7.77. For ^1H and ^{13}C NMR, see **Table 1**.

N-Ethylquinine (**5**). Amorphous; $[\alpha]^{25}_D$ + 128.0° (*c* 0.125, EtOH); IR (film) ν_{max}: 3224, 3075, 2935, 1620, 1591, 1472, 1433, 1241, 1229, 1135, 1104, 1028, 863, 832, 755 cm^{-1}; UV (EtOH) λ_{max} (log ϵ) 333 sh (2.17), 279 sh (2.14), 230 (3.02) nm; EIMS *m*/*z* $[M]^+$ 353 (1), 324 (100), 309 (7), 307 (3), 295 (2), 283 (4), 173 (10), 137 (9), 136 (45), 82 (2); HREIMS *m*/*z* $[M + 1]^+$ 353.1232 (calcd for $C_{22}H_{29}N_2O_2$ 353.2229). For ^1H and ^{13}C NMR, see **Table 1**.

RESULTS AND DISCUSSION

Five alkaloids (**1**−**5**) were isolated from the bark of *Remijia peruviana*. The new alkaloid **4** was an amorphous white powder. Its UV spectra showed bands at λ_{max} 338 (log ϵ, 2.48), 286 (log ϵ, 2.41), and 232 (log ϵ, 3.25). Its mass spectrum (EIMS) showed principal fragments at 324, 309, 294, and 136 amu, identical to quinine-type alkaloid derivatives (*20*). The molecular ion was not detected in fast atom bombardment (FAB) and EIMS experiments. However, the HREIMS showed a molecular ion peak at *m*/*z* 352.1775 (0.02) corresponding to the molecular formula $C_{21}H_{24}N_2O_3$. The ^{13}C NMR (DEPT experiments) showed 21 carbon atoms, 1 methyl, 5 methylenes, 10 methines, and 5 quaternary carbon atoms. The ^1H NMR spectra of alkaloids **4** and **5** in $CDCl_3$ were complex, with overlapping signals in the high field region at 500 MHz. The proton assignments of the quinoline moiety were established according to previous work (*21*); however, this is their first complete report (**Table 1**).

The proton signals of the quinuclidine ring of **4** were determined by 2D NMR experiments. Its COSY showed a signal proton at δ_H 4.17 assignable to H-6_{endo} coupled with the proton at δ_H 3.00 (ddd, H-6_{exo}) and with H-5_{endo} and H-5_{exo} at δ_H 1.74 (m) and 2.02 (m), respectively. Moreover, this proton gave a positive nuclear Overhauser effect (NOE) with the signal corresponding to the proton at δ_H 5.83 (s, H-9). Similarly, the signal at δ_H 3.36 (t, J = 8.6 Hz, H-8β) showed a spatial correlation with the protons at δ_H 3.10 (br d), 5.83 (s), 7.13

Table 1. ^{1}H, ^{13}C, HSQC, and HMBC NMR Data for Alkaloids **4** and **5**[a]

	4			**5**		
proton	$\delta_{\dot{H}}$ (J_{H-H} in Hz)	HSQC	HMBC	$\delta_{\dot{H}}$	HSQC	HMBC
H-2_{trans}	3.27 dd (13.3, 10.2)	54.2 (t)	C-3, C-6, C-8, C-10	3.28 m	48.2 (t)	C-8
H-2_{cis}	3.10 br d (13.7)		C-3, C-6, C-8, C-10	4.26 t (10.1)		C-3, C-6, C10
H-3	2.57 m	37.4 (d)	C-7, C-10	2.51 q (8.5)	37.7 (d)	C-2, C-4, C-5, C-7, C-10, C-11
H-4	1.96 m	26.8 (d)	C-3, C-5, C-8	1.94 m	27.6 (d)	
H-5_{exo}	1.74 m	24.5 (t)	C-4, C-7	1.84 m	23.8 (t)	C-7
H-5_{endo}	2.02 m		C-3	1.66 m		C-3, C-4
H-6_{exo}	3.00 ddd (11.8, 11.9,5.0)	43.6 (t)	C-8	3.08 m	48.9 (t)	C-8
H-6_{endo}	4.17 m		C-2	3.28 m		C-2, C-4
H-7_{exo}	1.22 m	18.3 (t)	C-5	2.32 t (11.8)	18.4 (t)	C-3, C-4, C-5, C-8, C-9
H-7_{endo}	1.96 m		C-3, C-5, C-9	0.95 m		C-3
H-8	3.36 t (8.6)	59.3 (d)	C-2, C-6, C-7, C-4′	3.28 m	59.8 (d)	C-4, C-6
H-9	5.83 s	66.8 (d)	C-3′, C-4′, C-7, C-8, C-10′	6.33 br s ($w_{1/2}$ = 8.9 Hz)	66.8 (d)	C-3′, C-4′, C-7, C-8, C-10′
H-10	5.53 ddd (17.1,10.4, 7.0)	137.8 (d)	C-2, C-3, C-4	6.03 ddd (16.6, 10.8, 7.5)	136.8 (d)	C-2, C-3
H-11_{cis}	4.98 d (17.2)	116.6 (t)	C-3, C-10	5.22 d (15.8)	117.2 (t)	C-3, C-10
H-11_{trans}	4.94 d (10.4)		C-3, C-10	5.21 d (11.6)		C-3, C-10
H-2′	8.55 d (4.5)	146.2 (d)	C-3′, C-4′, C-9′	8.72 d (4.4)	147.4 (d)	C-3′, C-4′
H-3′	7.57 d (4.6)	118.4 (d)	C-2′, C-9, C-10′	7.67 d (4.4)	121.7 (d)	C-9, C-10′
H-4′		144.7 (s)			144.5 (s)	
H-5′	7.13 d (2.6)	102.8 (d)	C-6′, C-7′, C-9′	7.04 br s	100.2 (d)	C-4′, C-6′, C-7′
H-6′		156.4 (s)			158.0 (s)	
H-7′	7.27 dd (9.1, 2.5)	122.5 (d)	C-5′, C-7′, C-9′	7.21 d (9.1)	118.7 (d)	C-5′, C-6′, C-9′
H-8′	7.88 d (9.1)	131.0 (d)	C-6′, C-10′	7.99 d (8.9)	131.6 (d)	C-6′, C-10′
H-9′		142.7 (s)			125.5 (s)	
H-10′		125.9 (s)			143.9 (s)	
OCH_3				3.81 s	55.9 (q)	C-6′
Me—C═O	1.98 s	179.6 (s)				
		23.4 (q)				
N—*CH_2*—CH_3				2.94 q (7.1)	42.2 (t)	N—CH_2—*CH_3*
N—CH_2—*CH_3*				1.29 t (7.0)	11.9 (q)	N—*CH_2*—CH_3

[a] NMR data in $CDCl_3$; 500 MHz.

Table 2. Scalar and Spatial Correlation, COSY and NOESY, for Alkaloids **4** and **5**

	4		**5**	
proton	COSY	NOESY	COSY	NOESY
H-2_{trans}	H-2_{cis}, H-3	H-2_{cis}, H-3, H-6_{exo}	H-2_{cis}, H-3	H-2_{cis} H-3, H-6_{exo}
H-2_{cis}	H-2_{trans}, H-3	H-2_{trans}, H-3, H-8β, H-11_{cis}, H-11_{trans}	H-2_{trans}, H-3	H-7, H-8β, H-10
H-3	H-2_{cis}, H-2_{trans}, H-4, H-10	H-2_{trans}, H-5_{exo}, H-10, H-11_{cis}, H-11_{trans}	H-2_{cis}, H-2_{trans}, H-10	H-2_{trans}, H-4, H-5_{exo}, H-6_{exo}, H-11_{cis}, H-11_{trans}
H-4	H-3, H-5_{exo}, H-5_{endo}, H-7	H-3	H-3	H-3, H-5_{endo}, H-7_{exo}, H-7_{endo}
H-5_{exo}	H-5_{endo}, H-6_{exo}, H-6_{endo}	H-3, H-5_{endo}, H-6_{exo}	H-5_{endo}, H-6_{exo}	H-3, H-5_{endo}, H-6_{exo}
H-5_{endo}	H-5_{exo}, H-6_{exo}, H-6_{endo}	H-5_{exo}, H-6_{exo}	H-5_{exo}, H-6_{endo}	H-4, H-5_{exo}, H-6_{endo}, H-7_{endo}
H-6_{exo}	H-5_{endo}, H-5_{exo}, H-6_{endo}	H-2_{trans}, H-5_{exo}, H-6_{endo}	H-5_{exo}, H-6_{endo}	H-3, H-5_{exo}, H-6_{endo}
H-6_{endo}	H-5_{endo}, H-5_{exo}, H-6_{exo}	H-5_{endo}, H-6_{exo}, H-9	H-5_{endo}, H-5_{exo}	H-5_{endo}, H-6_{exo}, H-7_{endo}
H-7_{exo}	H-4, H-7_{endo}, H-8	H-7_{endo}, H-8, H-10	H-7_{endo}, H-8	H-2_{cis}, H-3′, H-4, H-7_{endo}, H-10
H-7_{endo}	H-7_{exo}, H-8	H-7_{exo}, H-9	H-7_{exo}, H-8	H-4, H-5_{endo}, H-6_{endo}, H-7_{exo}
H-8	H-7_{exo}, H-7_{endo}	H-2_{cis}, H-7_{exo}, H-9, H-5′	H-7_{exo}, H-7_{endo}	H-2_{cis}, H-5′, H-9
H-9	H-8	H-5′, H-6_{endo}, H-7_{endo}, H-8		H-8, H-5′
H-10	H-3, H-11_{trans}, H-11_{cis}	H-2_{cis}, H-3, H-4, H-7_{exo}, H-11_{trans}, H-11_{cis}	H-3, H-11_{trans}, H-11_{cis}	H-2_{cis}, H-7_{exo}, H-11_{trans}, H-11_{cis}
H-11_{cis}	H-10	H-2_{cis}, H-3, H-10	H-10	H-3, H-10
H-11_{trans}	H-10	H-2_{cis}, H-3, H-10	H-10	H-3, H-10
H-2′	H-3′	H-3′	H-3′	H-3′
H-3′	H-2′	H-2′	H-2′	H-2′, H-7_{exo}
H-5′		H-8, H-9		H-8, H-9, OCH_3
H-7′	H-8′	H-8′	H-8′	H-8′, OCH_3
H-8′	H-7′	H-7′	H-7′	H-7′
OCH_3				H-5′, H-7′
CH_3—C═O		H-7′		
CH_3—NCH_2			N—CH_2—*CH_3*	N—CH_2—*CH_3*
			N—*CH_2*—CH_3	N—*CH_2*—CH_3

(d), and 1.22 (m) attributable to the protons H-2_{cis}, H-9, H-5′, and H-7_{exo}, respectively. Moreover, the singlet at δ_H 5.83 (H-9) coupled with H-8 in the COSY spectrum gave a NOE with the protons H-6_{endo} and H-5′ in the NOESY spectrum. Likewise, the vinyl proton at δ_H 5.53 (ddd, H-10) displayed scalar coupling with proton H-3 and with both terminal vinyl protons H-11_{cis} and H-11_{trans} in a COSY spectrum and spatial correlation with the proton signals H-7_{exo}, H-4, H-3, and H-2_{cis} (**Table 2**). HSQC and HMBC experiments confirmed the chemical shifts of an acetyl group located at C-6′. The remaining protons (**Table 1**) are in agreement with the proposed structure for alkaloid **4**. The data indicate that the orientation of quinuclidine with respect to the quinoline ring is such that H-8 is closer in space to H-5′, suggesting that the configuration of H-8 is an α-linkage (β-position) (*22*) and that the "closed conformation 2" must be present in alkaloid **4** (*23*).

Alkaloid **5**, an amorphous white powder, showed IR bands at 1620, 1591, 1509, 1229, and 755 cm^{-1} and UV absorption λ_{max} 333 (log ϵ, 2.17), 280 (log ϵ, 2.14), and 232 (log ϵ, 3.02), respectively. The HREIMS gave a molecular ion peak $[M]^+$ at *m*/*z* 353.2132 corresponding to the molecular formula $C_{22}H_{29}N_2O_2$. The NMR spectroscopic data of **5** were similar to

Table 3. NMR Data for Cupreine (**2**), Cinchonine (**3**), and Cinchonine–HCl

	2			**3**		cinchonine–HCl[a]	
proton	$\delta_{\dot{H}}$ (J_{H-H} in Hz)	HSQC	NOESY	$\delta_{\dot{H}}$[b]	HSQC	$\delta_{\dot{H}}$	HSQC
H-2_{trans}	2.99 t (10.8)	55.6 (t)	H-2_{cis}, H-3, H-6_{exo}	2.93 m	48.6 (t)	3.30 m	48.6 (t)
H-2_{cis}	2.72 d (11.0)		H-2_{trans}, H-3, H-8, H-10	3.38 m		4.34 m	
H-3	2.34 br s	38.6 (d)	H-2_{cis}, H-2_{trans}, H-5_{exo}, H-4, H-10, H-11	2.24 m	37.7 (d)	2.54 m	37.7 (d)
H-4	1.86 s	27.4 (d)	H-3, H-5_{exo}, H-7_{exo}, H-10	1.74 br s	27.6 (d)	2.03 br s	27.6 (d)
H-5_{cis}	1.57 s	26.1 (t)	H-3, H-4, H-6_{exo}	1.50 m	23.6 (t)	1.83 m	23.6 (t)
H-5_{trans}	1.96 m		H-6_{endo}			1.64 m	
H-6_{exo}	2.80 m	43.5 (t)	H-2_{trans}, H-5_{exo}	2.78 m	49.3 (t)	3.07 m	49.3 (t)
H-6_{endo}	4.10 br t (10.4)		H-5_{endo}, H-5′, H-9	2.93 m		3.40 br t (10.6)	
H-7_{exo}	1.26 m	18.6 (t)	H-4, H-8, H-10	1.50 m	18.2 (t)	2.34 m	18.2 (t)
H-7_{endo}	1.96 m		H-3, H-4, H-8, H-3′	1.14 m		0.95 m	
H-8	3.20 t (8.5)	59.4 (d)	H-2_{cis}, H-7_{exo}, H-9, H-10, H-5′	3.11 m	60.4 (d)	3.30 m	60.4 (d)
H-9	6.0 s	69.2 (d)	H-6_{endo}, H-8, H-5′	5.77 d (4.4)	66.8 (d)	6.52 br s	66.8 (d)
H-10	5.45 ddd (8.6, 9.8, 16.7)	139.8 (d)	H-2_{cis}, H-3, H-4, H-7_{exo}, H-8, H-11	5.91 ddd (7.1, 10.2, 17.8)	136.6 (d)	6.04 ddd (7.1, 10.2, 17.8)	136.6 (d)
H-11_{cis}	4.84 d (17.0)	115.4 (t)	H-3, H-10	5.00 d (16.3)	114.5 (t)	5.23 d (16.3)	117.5 (t)
H-11_{trans}	4.86 d (10.0)		H-3, H-10	4.98 d (11.2)		5.22 d (11.2)	
H-2′	8.52 d (3.9)	146.3 (d)	H-3′	8.84 d (4.5)	149.9 (d)	8.85 d (4.0)	149.9 (d)
H-3′	7.51 d (3.9)	117.8 (d)	H-2′, H-7_{endo}, H-8, H-9	7.56 d (4.5)	118.6 (d)	7.72 d (4.6)	118.6 (d)
H-4′		146.2 (s)			145.9 (s)		145.9 (s)
H-5′	7.37 s	103.3 (d)	H-6_{endo}, H-8, H-9	8.05 d (9.8)	122.3 (d)	7.93 d (8.1)	122.3 (d)
H-6′		157.0 (s)		7.44 t (8.5)	127.6 (d)	7.16 t (7.1)	127.0 (d)
H-7′	7.16 d (8.9)	122.9 (d)	H-8′	7.61 t (8.2)	128.9 (d)	7.45 t (7.6)	128.9 (d)
H-8′	7.80 d (8.9)	131.2 (d)	H-7′	7.96 d (7.4)	129.9 (d)	7.89 d (8.2)	129.9 (d)
H-9′		142.8 (s)			147.7 (s)		147.6 (s)
H-10′		126.2 (s)			124.4 (s)		124.4 (s)

[a] Reference 22. [b] NMR data in $CDCl_3$.

those obtained for **4**, except for the presence of additional signals at δ_H 3.81 (s, 3H); δ_C 55.8 (q) and δ_H 2.92 (2H, q); and 1.29 (3H, t), δ_C 42.2 (t), and 11.8 (q), assignable to a methoxy and to an *N*-ethyl group. The methoxy group was located in the quinoline moiety at C-6′ (HSQC and HMBC experiments) and the ethyl group at the quinuclidine nitrogen. For this reason, the proton signal at δ_H 4.26 (t) was assignable to the H-2_{cis} vicinal to the quinuclidine nitrogen atom and was displayed downfield showing a NOE with the signals corresponding to the protons at H-7_{exo}, H-8β, and H-10. Likewise, protons H-8β, H-6_{endo}, and H-9 exhibited a spatial correlation with the signal at δ_H 7.04 (br s, H-5′) that confirmed the same configuration for **5** as for alkaloid **4** (**Tables 1** and **2**). Alkaloid **1** was identified as quinine−hydrochloride and probably formed as a result of the extraction procedure, on the basis of its NMR data (*21*). Alkaloids **2** and **3** were the known alkaloids cupreine and cinchonine, previously isolated from *Remijia pedunculata* (*24*) and *Cinchona officinalis* (*25*), respectively. Complete NMR 1D and 2D data are presented for alkaloids **2** and **3** in this paper, because these data suggest that cupreine adopts the same closed conformation 2 as alkaloid **4**.

The antifeedant effects of the test compounds were specific and structure-dependent (**Table 4**). None of them affected the feeding behavior of *S. littoralis*, while *L. decemlineata* showed the strongest response to **3** (with 8*R*, 9*S* configuration) followed by **4** and **2** (with 8*S*, 9*R* configuration), suggesting that the stereochemistry and/or the substituents at C-6′ determined the antifeedant activity of these alkaloids. Quinoline-type alkaloids have been found to be an antifeedant/deterrent to some insect species. Quinine−HCl affected blowfly feeding behavior, acting on the sugar receptors (*26*). However, this is the first report of the insect antifeedant effects of **2**−**4**.

Orally injected *S. littoralis* larvae were not affected by the test compounds in short-term experiments (**Table 4**). Quinidine, quinine (**1**), and cinchonidine affected *S. littoralis* larvae in long-term chronic exposure experiments, and this was attributable to feeding deterrency (*27*). Therefore, the results shown here do not rule out any possible chronic effects of the test alkaloids.

Table 4. Effective Antifeedant Doses (EC_{50}) and 95% Confidence Limits (Lower, Upper) of the Test Compounds on *S. littoralis* L6 Larvae and Adult *L. decemlineata*[a]

		S. littoralis		
compound	*L. decemlineata* EC_{50} (μg/cm^2)	EC_{50} (μg/cm^2)	ΔI (% of control)	ΔB (% of control)
1	>50	>50	87	82
2	11.6 (2.4, 15.6)	≈50	98	98
3	1.8 (0.6, 4.9)	>50	106	113
3–HCl		>50	108	115
4	6.2 (2.4, 16.1)	>50	85	85

[a] Consumption (ΔI) and biomass gain (ΔB) of orally injected *S. littoralis* larvae.

Table 5. Cytotoxic and Trypanocidal Effects of the Test Compounds on Sf9 and CHO Cells and *T. cruzi*

	ED_{50}[a] (μg/mL)		
compound	Sf9	CHO	*T. cruzi*
1	>100	>100	≅50
2	>100	>100	>100
3	>100	>100	>100
3–HCl	7.4 (4.2, 13.0)[b]	>100	>100
4	32.4 (22.3,47.1)[b]	14.3 (5.9, 34.2)[b]	>100

[a] ED_{50} = concentration needed to produce 50% viability. [b] 95% confidence limits.

Alkaloid **4** was cytotoxic to both mammalian and insect cell lines after 48 h of incubation, and **3**−HCl had the strongest selective cytotoxic effects to Sf9. Cinchonine (**3**) was inactive under these assay conditions, indicating that the presence of the HCl molecule enhanced the short-term bioavailability of this compound to the insect cells (**Table 5**). This cytotoxicity indicates a toxic mode of action other than the neuroreceptor-mediated effects suggested by their antifeedant activity, since these cell lines are not related to neurotransmission. The selectivity of **3**−HCl between insect (Sf9) and mammal (CHO) cells might be related to differences in membrane composition. It has been shown that plasma membranes of Sf9 cells contain

Table 6. Cytotoxic Effects of the Test Compounds on Tumoral Cell Lines CT26, SW480, HeLa, SkMel25, and SkMel28

	ED_{50}[a] (μg/mL)					
compound	CHO	CT26	SW480	HeLa	SkMel25	SkMel28
1	32.5 (19.6, 53.8)	10.8 (7.1, 16.5)	62.1 (46.6, 82.9)	34.7 (19.3, 62.7)	48.0 (38.1, 60.4)	37.0 (25.5, 35.2)
2	33.5 (42.0, 110.0)	45.0 (31.7, 64.1)	40.5 (33.3, 49.3)	38.9 (35.0, 43.1)	24.3 (20.9, 28.1)	30.0 (4.2, 15.4)
3	0.5 (0.1, 1.7)	27.1 (22.6, 32.6)	22.6 (16.7, 30.5)	1.4 (0.8, 2.3)	13.0 (8.4, 19.9)	34.2 (22.7, 51.5)
3–HCl	2.7 (1.9, 4.0)	5.3 (2.3, 11.9)	4.9 (2.1, 11.3)	1.2 (0.8, 1.8)	4.3 (3.2, 5.7)	0.6 (0.2, 1.5)
4	4.8 (2.9, 7.9)	6.1 (3.2, 11.7)	2.50 (1.4, 4.3)	2.3 (1.3, 4.2)	2.7 (1.8, 4.1)	5.3 (3.0, 9.1)

[a] ED_{50} = concentration needed to produce 50% cell viability.

10 times less cholesterol than membranes isolated from mammalian cells, and the cholesterol-to-phospholipid ratio in Sf9 cells is lower than that in mammalian cells (*28*). These cytotoxic compounds did not affect orally injected *S. littoralis* larvae, thus suggesting metabolic detoxification, excretion, or target-site insensitivity.

T. cruzi was moderately affected by quinine (**1**) (**Table 5**). *Cinchona* alkaloids such as quinine (**1**), cinchonine (**3**), quinidine, and cinchonidine have been used as effective antimalarial drugs (*29*). Furthermore, these compounds have been reported as trypanocidal against bloodstream forms of the African *T. brucei* and *T. congolensis* (*30*). In this study, however, only **1** affected *T. cruzi*, suggesting species dependency for the trypanocidal effects of these alkaloids. Similarly, *T. congolensis* was less susceptible than *T. brucei* to quinoline alkaloids (*30*).

Table 6 shows the long-term effects of the test alkaloids on CHO cells and a panel of tumoral cell lines. Overall, the new alkaloids **4** and **3**−HCl were the most cytotoxic. Alkaloid **3** was less cytotoxic than **3**−HCl for all of the cell lines except the CHO cells, suggesting a selective, delayed effect of **3** on this cell line. In terms of selective cytotoxicity (tumoral/CHO cells), **3**−HCl (SkMel28, 4.5-fold; HeLa, 2-fold) and **1** (CT26, 3-fold) were the most selective, followed by **4** (SW480, HeLa, and SkMel25, 2-fold) and **2** (SkMel25, 1.4-fold). Several factors, such as intracellular transportation, metabolism, and inactivation and receptor geometry, may contribute to this differential mode of action. Similarly, quinine (**1**) and cinchonine (**3**), among other related alkaloids, have been reported to be cytotoxic to human HL-60 cells (*31*). Overall, the predicted (SW480 > CT26, SKMel28, HeLa > SKMel25) and observed resistance of the tumoral cell lines did not correlate, especially for the effects of **4** and **3**−HCl. The lack of resistance of SW480, CT26, and SKMel28 cells to these compounds could be related to the inhibition of the resistance mechanism. Cinchonine (**3**) partially reversed the drug resistance of tumoral cells more efficiently than quinine (**1**) through Pgp binding (*31*).

The cytotoxic action of these alkaloids showed similar structural requirements to the antifeedant effects (8*R*, 9*S* conformation or acetylation at C-6′ for the 8*S*, 9*R* alkaloids). Similarly, the relative "in vitro" antimalarial activity of **1** and related substances has been established with the 8*R*, 9*S* conformation having the strongest activity (*32*). These generalized conformational requirements suggest a common mechanism for the molecular interactions involved in the diverse biological activities found for these alkaloids.

Alkaloids are considered to be multipurpose defense substances because of their wide-ranging activities concerning their multiple-target actions. Specifically, quinoline-type alkaloids inhibit protein biosynthesis, intercalate with DNA, affect DNA polymerase I and reverse transcriptase (**1**, **3**, cinchonidine, and quinidine), and bind to nicotinic and muscarinic neuroreceptors (**1**), adrenergic neuroreceptors (**3**, **1**, cinchonidine, and quinidine), and serotonin neuroreceptors (*33*). Therefore, the antifeedant effects of alkaloids **2**−**4** could be related to neuroreceptor binding activities, according to the neuroreceptor-mediated insect-taste regulation hypothesis (*34*), while their cytotoxicity is probably due to DNA damage and/or protein biosynthesis inhibition, assuming that binding to these molecular targets involves similar molecular interactions that could explain different biological activities with similar structural requirements as suggested (*33*).

ABBREVIATIONS USED

Sf9, *S. frugiperda* pupal ovarian tissue cells; CHO, chinese hamster ovary; CT26, murine colon adenocarcinoma; SW480, human colon adenocarcinoma; HeLa, human cervical adenocarcinoma; SkMel25, human melanoma; SkMel28, human malignant melanoma; Pgp, P-glycoprotein; MRP1, multidrug-resistance protein; GSH/GST, the murine glutathione/glutathione *S*-transferase detoxification system; FBS, fetal bovine serum; MTT, 3-[4,5-dimethylthiazol-2-yl]-2,5-diphenyl-tetrazolium bromide.

ACKNOWLEDGMENT

We gratefully acknowledge S. Carlin for language revision.

Supporting Information Available: Quinine (**1**). Resin; EIMS *m/z* $[M]^+$ 324 (1), 309(1), 296 (1), 233 (1), 205 (6), 189 (5), 137 (10), 136 (100), 91 (78), 81 (7); HREIMS *m/z* $[M]^+$ 324.1831 (calcd for $C_{20}H_{24}N_2O_2$ 324.1837); ^{1}H NMR (HCl form, $CDCl_3$, 500 MHz) δ_H 8.62 (H, d, J = 4.5 Hz, H-2′), 7.45 (H, br s, H-5′), 7.90 (H, d, J = 8.0 Hz, H-8′), 7.31 (H, d, J = 8.0 Hz, H-7′), 7.70 (H, d, J = 4.5 Hz, H-3′), 5.60 (H, ddd, J = 7.1, 10.2, 17.8 Hz, H-10), 6.40 (H, brd, J = 4.4 Hz, H-9), 5.10 (H, d, J = 16.3 Hz, H-J = 11a), 4.97 (H, d, J = 11.2 Hz, H-11b), 4.10 (H, m, H-6_{endo}), 4.03 (3H, s, OCH_3), 3.32 (H, dd, J = 13.2, 10.0 Hz, H-2_{trans}), 3.31 (H, m, H-8), 3.10 (2H, m, H-2_{cis} and H-6_{exo}), 2.47 (H, m, H-3), 2.11 (H, m, H-5_{endo}), 2.05 (H, br s, H-4), 1.82 (H, m, H-5_{exo}), 1.34 and 0.79 (H each, m, H-7_{endo} and H-7_{exo}, respectively). Cupreine (**2**). Oil; $[\alpha]^{25}_D$ − 130.23° (*c* 0.655, EtOH); UV (EtOH) λ_{max} (log ϵ) 336 sh (1.2) nm, 233 sh (2.0) nm; EIMS *m/z* $[M]^+$ 310 (3), 309(1), 238 (1), 200 (2), 188 (6), 175 (20), 159(17), 146 (21), 137 (35), 136 (100), 81 (33); HREIMS *m/z* $[M]^+$ 310.1629 (calcd for $C_{19}H_{22}N_2O_2$ 310.1681). Cinchonine (**3**). Crystallized from CH_2Cl_2−MeOH; mp 256−57 °C; $[\alpha]^{25}_D$ + 230° (*c* 0.64, EtOH); [lit. mp 260 °C, and $[\alpha]^{25}_D$ + 224 (EtOH), respectively] (*17*); IR (film) ν_{max}: 3110, 2918, 1654, 1560, 1508, 1458, 1108, 995, 761 cm^{-1}; UV (EtOH) λ_{max} (log ϵ) 314 sh (4.0) nm, 284 sh (3.2) nm, 225 (3.9) nm; EIMS *m/z* $[M]^+$ 294 (25), 253 (7), 159 (17), 143 (11), 136 (100), 130 (11), 108 (5), 95 (7), 85 (11), 83 (17), 81 (17), 55 (11); HREIMS *m/z* $[M]^+$ 294.1684 (calcd for $C_{19}H_{22}N_2O$ 294.1732). For ^{1}H and ^{13}C NMR, see **Table 3**. This material is available free of charge via the Internet at http://pubs.acs.org.

LITERATURE CITED

(1) Verpoorte, R.; Scripsema, J.; Van der Leer, T. In *The Alkaloids*; Brossi, A., Ed.; Academic Press: San Diego, CA, 1988; Vol. 34, pp 332−398.

(2) Grethe, G.; Uskokovic, M. R. *Heterocyclic Compounds*. *The Monoterpenoid Indole Alkaloids*; John Wiley and Sons Inc.: New York, 1983; Vol. 25, Part 4, p 729 and references therein.

(3) Prelog, V. Relative configuration of carbon atoms 8 and 9 of Cinchona alkaloids. *Tetrahedron Lett.* **1964**, 2037−2038.

(4) Madhusudanan, K. P.; Pratap, R.; Popli, S. P. Steric influence on chemical ionization mass spectra of Cinchona alkaloids. *Ind. J. Chem*. **1985**, *24B*, 67−70.

(5) Ramírez-Sosa, C. R.; Rengifo, E.; Morey, K. Z. Market Medicinal Plants in El Salvador and Amazonian Peru: a Comparison Study. Presented at the International Colloquium on Medicinal and Aromatic Plants, Health, Conservation and the Environment, Rabat, Morocco, 2002.

(6) Dong, Z.; Radinsky, R.; Fan, D.; Tsan, R.; Bucana, C. D.; Wilmanns, C.; Fidler, I. J. Organ-specific modulation of steady-state mdr gene expression and drug resistance in murine colon cancer cells. *J. Natl. Cancer Inst*. **1994**, *86*, 913−920.

(7) Xiao, B.; Singh, S. P.; Nanduri, B.; Awasthi, Y. C.; Zimniak, P.; Ji, X. Crystal structure of a murine glutathione S-transferase in complex with a glutathione conjugate of 4-hydroxynon-2-enal in one subunit and glutathione in the other: evidence of signaling across the dimer interface *Biochemistry* **1999**, *38*, 11887−11894.

(8) Iwahashi, T.; Okochi, E.; Ariyoshi, K.; Watabe, H.; Amann, E.; Mori, S.; Tsuruo, T.; Ono, K. Specific targeting and killing activities of anti-P-glycoprotein monoclonal antibody MRK16 directed against intrinsically multidrug-resistant human colorectal carcinoma cell lines in the nude mouse model. *Cancer Res*. **1993**, *53*, 5475−5482.

(9) Lin-Lee, Y. C.; Tatebe, S.; Savaraj, N.; Ishikawa, T.; Kuo, M. T. Differential sensitivities of the *MRP* gene family and γ-glutamylcysteine synthetase to prooxidants in human colorectal carcinoma cell lines with different p53 status. *Biochem. Pharmacol*. **2001**, *61*, 555−563.

(10) de Bittencourt, P. I.; Curi, R.; Williams, J. F. Glutathione metabolism and glutathione S-conjugate export ATPase (MRP1/GS-X pump) activity in cancer. I. Differential expression in human cancer cell lines. *Biochem. Mol. Biol. Int*. **1998**, *45*, 1227−1241.

(11) Suter, L.; Bruggen, J.; Brocker, E. B.; Sorg, C. A. A tumor-associated antigen expressed in melanoma cells with lower malignant potential. *Int. J. Cancer* **1985**, *35*, 787−791.

(12) Alvino, E.; Gilberti, S.; Cantagallo, D.; Massoud, R.; Gatteschi, A.; Tentori, L.; Bonmassar, E.; D'Atri, S. In vitro antitumor activity of 3′-desamino-3′(2-methoxy-4-morpholinyl) doxorubicin on human melanoma cells sensitive or resistant to triazene compounds. *Cancer Chemother. Pharmacol*. **1997**, *40*, 180−184.

(13) Berger, W.; Hauptmann, E.; Elbling, L.; Vetterlein, M.; Kokoschka, E. M.; Micksche, M. Possible role of the multidrug resistance-associated protein (MRP) in chemoresistance of human melanoma cells *Int. J. Cancer* **1997**, *71*, 108−115.

(14) Reina, M.; González-Coloma, A.; Gutiérrez, C.; Cabrera, R.; Rodriguez, M. L.; Fajardo, V.; Villarroel, L. Defensive Chemistry of *Senecio miser Hook. J. Nat. Prod*. **2001**, *64*, 6−11.

(15) González-Coloma, A.; Guadaño, A.; De Inés, C.; Martinez-Díaz, R.; Cortes, D. Selective action of acetogenin mitochondrial Complex I inhibitors. *Z. Naturforsch*. **2002**, *57c*, 1028−1034.

(16) Muelas-Serrano, S.; Nogal-Ruiz, J. J.; Gómez-Barrio, A. Setting of a colorimetric method to determine the viability of *Trypanosoma cruzi* epimastigotes. *Parasitol. Res*. **2000**, *86*, 999−1002.

(17) Mossman, T. Rapid colorimetric assay for cellular growth and survival: Application to proliferation and cytotoxicity assays *J. Immunol. Methods* **1983**, *65*, 55−63.

(18) Berridge, M. V.; Tan, A. S. Characterizarion of the cellular reduction of 3-(4,5-dimethylthiazol-2-yl)-2,5-diphenyltetrazolium bromide (MTT): subcellular localization, substrate dependence and involvement of mitochondrial electron transport in MTT reduction. *Arch. Biochem. Biophys*. **1993**, *303*, 474−482.

(19) Liu, Y.; Peterson, D. A.: Kimura, H.; Schubert, D. Mechanism of cellular 3-(4,5-dimethylthiazol-2-yl)-2,5-diphenyltetrazolium bromide (MTT) reduction. *J. Neurochem*. **1997**, *69*, 581−593.

(20) Bartók, T.; Szöllösi, K.; Bartok, M.; Thiel, J. New results on the mass spectra of Cinchona alkaloids. *J. Mass Spectrom*. **2000**, *35*, 711−717.

(21) Prakash, O. M.; Roy, R.; Singh, I. P.; Pratp, R.; Poplip, S. P.; Bhakuni, D. S. Steric influence on high resolution ^{1}H NMR spectra of Cinchona alkaloids. *Ind. J. Chem*. **1988**, *27B*, 950−952.

(22) Chazin W. J.; Colebrook. L. D. Use of Proton Spin−Lattice Relaxation and Nuclear Overhauser Effect Data in Structure Analysis of Alkaloids. *J. Org. Chem*. **1986**, *51*, 1243−1253.

(23) Dijkstra, G. D. H.; Kellogg, R. M.; Wynberg, H. Conformational Study of Cinchona Alkaloids. Combined NMR and Molecular Orbital Approach. *J. Org. Chem*. **1990**, *55*, 6121−6131.

(24) Hesse, O. Zur Geschichte der Cuprearinde. *Ber*. **1883**, *16*, 58−63.

(25) Lyle, G. G.; Keefer, L. K. The configurations at C-9 of the Cinchona alkaloids. NMR spectral study of the derived oxiranes. *Tetrahedron* **1967**, *23*, 3253−3263.

(26) Dethier, V. G.; Bowdan, E. The effect of alkaloids on sugar receptors and the feeding behavior of the blowfly. *Physiol. Entomol*. **1989**, *14*, 127−136.

(27) Krug, E.; Proksch, P. Influence of dietary alkaloids on survival and growth of *Spodoptera littoralis*. *Biochem. Syst. Ecol*. **1993**, *21*, 749−756.

(28) Marheineke K.; Grünewald, S.; Christie, W.; Reiländer, H. Lipid composition of *Spodoptera frugiperda* (Sf9) and *Trichoplusia ni* (Tn) insect cells used for baculovirus infection. *FEBS Lett.* **1998**, *441*, 49−52.

(29) Barennes, H.; Kahiatani, F.; Pussard, E.; Clavier, F.; Maeynard, D.; Njifountawouo, S.; Verdier, F. Intrarectal Quinimax (an association of Cinchona alkaloids) for the treatment of *Plasmodium falciparum* malaria in children in Niger: efficacy and pharmacokinetics. *Trans. R. Soc. Trop. Med. Hyg*. **1995**, *89*, 418−421.

(30) Merschjohann, K.; Sporer, F.; Steverding, D.; Wink, M. In vitro effect of alkaloids on Bloodstream forms of *Trypanosoma brucei* and *T. congolense*. *Planta Med*. **2001**, *67*, 623−627.

(31) Furusawa, S.; Nakano, S.; Wu, J.; Sagakuchi, S.; Takayanagi, M.; Saski, K.-I.; Satoh, S. Apoptosis induced by doxorubicin and cinchonine in P388 multidrug-resistant cells. *J. Pharm. Chemother*. **1992**, *36*, 1538−1544.

(32) Karle, J. M.; Karle, I. L.; Gerena, L.; Milhous, W. K. Stereochemical evaluation of the relative activities of the Cinchona alkaloids against *Plasmodium falciparum*. *Antimicrob. Agents Pharmacol*. **2001**, *53*, 1029−1039.

(33) Wink, M.; Schmeller, T.; Latz-Brüning, B. Modes of Action of Allelochemical Alkaloids: Interaction with Neuroreceptors, DNA, and Other Molecular Targets. *J. Chem. Ecol*. **1998**, *24*, 1881−1937.

(34) Mullin, C. A.; Chyb, S.; Eichenseer, H.; Hollister, B.; Frazier, J. L. Neuroreceptor mechanisms in insect gustation: a pharmacological approach. *J. Insect Physiol*. **1994**, *40*, 913−931.

Received for review July 7, 2004. Revised manuscript received October 21, 2004. Accepted November 11, 2004. This work was partially supported by grants MCYT (BQU2001-1505), CAM (07M/0073/2002), CYTED IV.13, Proyecto Vigía (Instituto Nacional de Salud, Lima, Peru), CYTED X (Convenio Andrés Bello, Química Fina y Farmaceútica), and a CAM-postdoctoral fellowship to C.d.I.

JF048880E